L-subshell ionization cross sections for proton bombardment of Ag, In, Sn, and I

E. Rosato
Istituto di Fisica Sperimentale, Università degli Studi di Napoli, I-80125 Napoli, Italy
and Istituto Nazionale di Fisica Nucleare, Sezione di Napoli, I-80125 Napoli, Italy
(Received 5 April 1983)

L-x-ray production cross sections were measured for thin targets of Ag, In, Sn, and I in the proton energy range 0.300–5.000 MeV. Subshell ionization cross sections were extracted and compared with existing data and with the predictions of plane-wave Born approximation (PWBA), perturbed–stationary-state theory including energy loss, Coulomb deflection and relativistic corrections (ECPSSR), binary-encounter approximation with corrections accounting for binding effect and Coulomb retardation (BEABC), and semiclassical approximation taking into account binding, energy loss, Coulomb deflection, and relativistic effects (SCABCR). Large disagreement was found with PWBA, but the other theories reproduced the experimental data rather well. Owing to the nodal structure of the $2s$ wave function, deeper insight was achieved by considering the ratios of the subshell ionization cross sections. These results were found to be in good agreement with analogous measurements on high-Z elements and favor the ECPSSR over the other theories. A realistic value for the ω_1 fluorescence yield was suggested for indium near the discontinuity at $Z \sim 50$.

I. INTRODUCTION

In recent years much effort has been devoted to the investigation of atomic inner-shell ionization by charged particles.[1–5] Consequently, there is now a large amount of experimental information on ionization cross sections over nearly the entire periodic table, mainly for the K shell.[6–8] This has stimulated theoretical research giving rise to several models for describing the ionization process, i.e., plane-wave Born approximation (PWBA),[9] perturbed–stationary-state theory (PSS),[10] binary-encounter approximation (BEA),[11,12] and semiclassical approximation (SCA).[13] Generally the magnitude and the overall trend of the experimental data are well reproduced, but large discrepancies still exist, especially for low-velocity bombarding particles. Therefore, corrections have been introduced in order to account for the perturbation of the target atom produced by the incoming particle, the projectile deflection due to the nuclear Coulomb field, the relativistic motion of the inner-shell electrons, and the energy loss of the ionizing particle.

With regard to the K shell, the measured data are becoming more and more accurate, thus making possible stringent tests of current theories. The experimental results are quite well reproduced by the above-mentioned models with the various corrections included, particularly by the perturbed–stationary-state theory with energy loss, Coulomb deflection, and relativistic corrections (ECPSSR),[6] apart from an underestimation of the Coulomb deflection factor at low velocity.[7,8]

The situation is somewhat involved in the case of L-shell ionization. First, the available data are rather scarce, the measurements have been confined mostly to the high-Z region, and the results from different authors often show large disagreements with each other. Second, for light and medium elements, the finite resolution of dispersive spectrometers makes it impossible to resolve the contributions from the different L lines and, consequently, to extract the L-subshell ionization cross sections. Even when this separation can be achieved, this task is not simple owing to the atomic parameters which connect the x-ray production cross sections to the ionization ones, i.e., fluorescence yields, Coster-Kronig (CK) rates, and radiative widths. These quantities cannot be easily measured and, therefore, phenomenological and/or theoretical estimates are commonly used.[14] Moreover, some of these parameters show sharp discontinuities for certain Z values because of the onset or cutoff of some CK transitions. This effect is noticeable around $Z \simeq 50$ since, in this region, the L_1-$L_3M_{4,5}$ transition becomes energetically forbidden while the L_1-$L_2M_{3,4}$ one turns out to be allowed.[15,16]

In the past only total L-shell measurements have been reported, except for the relative and indirect results of Ref. 62 concerning the ratios of Ag L-subshell ionization cross sections. In particular, the x-ray emission following proton-induced L-shell ionization has been extensively investigated in the case of silver and tin. On the contrary, the available iodine data reduce to a unique series of measurements, whereas in the case of indium, experimental results do not exist at all. The available experimental information is briefly summarized in Table I.

In the present work the energy range was extended down to $E_p = 0.300$ MeV in order to match the region of the characteristic inflection in the L_1 ionization cross section. This typical behavior is predicted by theory and can be ascribed to the electron density distribution inside the $2s$ orbital.[17] Thus, the comparison between experimental results and theoretical predictions can provide more detailed information about electronic wave functions and a more stringent test among the different models.

TABLE I. Summary of the available data concerning the total L-shell ionization cross sections of the elements investigated in the present work.

Element	Data	E_p (MeV)	Reference
Ag	103	0.120–40.000	22, 23, 24, 26, 36, 44, 48, 53, 54
In	none		
Sn	59	0.667–40.000	33, 35, 36, 44, 49, 53
I	5	3.000–11.000	44

II. EXPERIMENTAL METHODS

A. Apparatus

The experiment was carried out at the TTT-3 Tandem Accelerator of the University of Naples in the energy range $0.600 \leq E_p \leq 5.000$ MeV; for lower energies the AN-2000 Van de Graaff accelerator of Laboratori Nazionali di Legnaro (Padua) was used. In both cases the same type of scattering chamber was used with a graphite collimator and a Faraday cup at the ends. The proton beam was focused onto targets placed at 45° with respect to its axis. Thin targets were prepared by vacuum evaporation of Ag, In, and Sn onto 20-μg/cm^2-thick carbon backings. Iodine targets were obtained by evaporation of $AgIO_3$ aqueous solutions on the same backings. Rutherford backscattering analysis with 4.000-MeV $^4He^{2+}$ was performed before and after x-ray runs to measure the target thicknesses and to check the $AgIO_3$ stoichiometry. In all cases the targets turned out to be $\sim$20- to 30-μg/cm^2 thick, small enough to avoid self-absorption of the x rays and slowing down of the incident protons.

Si(Li) detectors, 170-eV resolution at 5.9 keV, were mounted at 90° with respect to the beam and located outside the vacuum system directly below the target. Kapton foils 25-μm thick were inserted as the chamber window in order to prevent the scattered protons from impinging onto the detectors and to avoid radiation damage. Beam currents were kept sufficiently low to reduce the x-ray counting rate in order to avoid pileup and lower electronic dead time.

B. Efficiency calibration

No calibrated sources are available for the low-energy L lines concerned in this work. Furthermore, measuring the Si(Li) detector efficiency in this region is an intricate problem owing to the steepest slope of the curve. Usually it is extracted by taking into account the absorption in the Be window, the Au contact, the Si dead layer, and possibly the chamber window and the air gap.[18] Here an indirect method was devised for evaluating the efficiencies at these low energies.

Firstly, the K-line efficiencies were measured for all the concerned elements. This was performed by using standard calibrated sources (^{54}Mn, ^{55}Fe, ^{57}Co, ^{65}Zn, ^{93m}Nb, ^{109}Cd, ^{137}Cs, and ^{241}Am manufactured by the Laboratoire de Métrologie des Rayonnements Ionisants-Paris) in the same geometry as in the actual measurements, following the procedure described in the literature.[19] Afterwards the K and L yields of Ag, Sn, and I were simultaneously measured and their ratios extracted at the proton energies where both K and L cross sections were available in tabular form.[13,20–55] Reference values of the x-ray production cross sections versus proton energy were obtained by performing weighted fits to the literature data by orthonormal polynomials.[56]

Secondly, statistical consistency among the various series of measurements from different authors was checked by means of a variance-ratio test.[57] In all the cases considered, the data turned out to be consistent except for the L-shell cross sections of Ag. In this case two sets of series of measurements can be picked out—the first for $E_p < 1.0$ MeV and the other for $E_p \geq 2.0$ MeV—internally consistent but with a large discrepancy between them. Thus, a choice became necessary. Better agreement with theoretical predictions was the discriminating criterion, leading to the rejection of the values from Refs. 26 and 36, which are much higher than the theoretical estimates.

Finally, the efficiency values were obtained from the relationship

$$\epsilon(\bar{E}_L) = \frac{\sigma_K}{\sigma_L} \frac{A_L}{\dfrac{A_{K\alpha}}{\epsilon(E_{K\alpha})} + \dfrac{A_{K\beta}}{\epsilon(E_{K\beta})}} , \tag{1}$$

where the ϵ are efficiencies; the σ, x-ray production cross sections; the A, peak areas; and the E, x-line energies (the weighted mean was taken for the L shell assuming as weights the intensity ratios of the different lines[58]). Obviously these values include solid-angle factors and intrinsically account for the x-ray attenuation through the chamber window and the air gap. The needed efficiencies for single L lines $\epsilon(E_{L_\nu})$ were extracted by interpolating an orthonormal polynomial fit[56] to the overall measured data. Further details about this procedure will be given in a forthcoming paper.[59]

C. Data analysis

The complex x-ray spectra were decomposed in Gaussian curves with automatic subtraction of continuous background[60] in order to extract the peak areas; an example of this analysis is shown in Fig. 1. Preliminary peeling of the spectra was performed for eliminating the background due to the K yields of low-Z contaminants (Cl, Ca, etc.) which superimposes to the investigated L lines. To this end spectra from blank backings (extracted from the same carbon foils used for the actual targets and bombarded with the same integrated beam charge) were subtracted from the target spectra.

Absolute L—x-ray production cross sections were obtained by

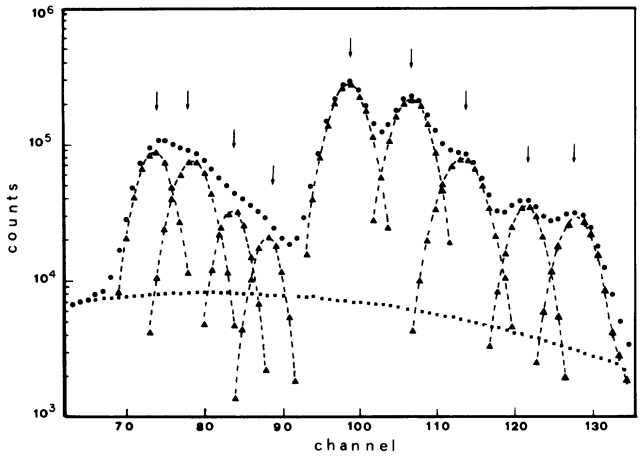

FIG. 1. Typical L—x-ray spectrum from $E_p=3.0$-MeV proton bombardment of $AgIO_3$: ●, experimental points; ■ calculated background; ▲, fitted Gauss curves. The analyzed peaks whose centroids are denoted by vertical arrows are, from left to right, $AgL\alpha_{1,2}$, $AgL\beta$, $AgL\beta_{2,15}$, $AgL\gamma_{1,5}$, $IL\alpha_{1,2}$, $IL\beta$, $IL\beta_{2,15}$, $IL\gamma_{1,5}$, and $IL\gamma_{2,3}$. The $L\beta$ lines are a mixture of $L\beta_1$, $L\beta_{3,4}$, and $L\beta_6$ contributions.

$$\sigma_{L\nu}=\frac{A_{L\nu}}{\epsilon(E_{L\nu})}\frac{\sigma_K}{\dfrac{A_{K\alpha}}{\epsilon(E_{K\alpha})}+\dfrac{A_{K\beta}}{\epsilon(E_{K\beta})}}\ , \tag{2}$$

where ν specifies the various L lines and the meaning of the other symbols is the same as in Eq. (1). All L and K quantities refer to the same element except for iodine whose L yield was normalized to the K yield of silver since its cross sections are better measured and the two elements have a well-defined stoichiometric ratio in $AgIO_3$. The reference cross sections were just the same and were obtained during the efficiency calibration procedure. Normalization to experimental cross sections rather than to theoretical estimates (essentially ECPSSR) was preferred because at low bombarding energies the theoretical predictions are too high owing to an underestimation of the Coulomb correction factor.[7,8]

Normalizing by simultaneous Rutherford scattering measurements was discarded for the following reasons: Several resonances appear in the $p+{}^{12}C$ reaction in the present energy range, appreciable amounts of contaminants are present in the backings, and important deviations from Rutherford law occur due to the electronic screening and/or the presence of nuclear effects. In any case, this method would require a separate determination of the particle-detector solid angle, thus introducing further uncertainty.

On the contrary, in the framework of the above-mentioned procedure, there is no need at all to account for the solid angle subtended by the x-ray detector, the target thickness, and the integrated beam charge, so the nonstatistical uncertainties they produce are completely canceled out. Therefore, the main source of error lies with the low K-yield counting statistics, especially for the lowest bombarding energies. Moreover, in this case, some additional contribution arises from the broadening of the confidence band in the reference K-shell cross sections. The resulting total uncertainty is $\sim 10\%$ in the worst case and much better for the highest energies.

L-subshell ionization cross sections σ_i were extracted from the following relationships:

$$\begin{aligned}\sigma_{L\alpha}&=[(f_{13}+f_{12}f_{23})\sigma_1+f_{23}\sigma_2+\sigma_3]\omega_3\frac{\Gamma_{L\alpha}}{\Gamma_3}\ ,\\ \sigma_{L\gamma_{1,5}}&=(f_{12}\sigma_1+\sigma_2)\omega_2\frac{\Gamma_{L\gamma_{1,5}}}{\Gamma_2}\ ,\\ \sigma_{L\gamma_{2,3}}&=\sigma_1\omega_1\frac{\Gamma_{L\gamma_{2,3}}}{\Gamma_1}\ ,\end{aligned} \tag{3}$$

where the f_{ij} are CK rates, the ω fluorescence yields, and the Γ radiative widths. The relativistic calculations by Scofield[60] were used for the radiative widths, and the values of f_{ij} and ω_i were taken from the compilation of Krause.[14] The theoretical estimates of Ref. 16 for ω_i and f_{ij} systematically produced $\sim 10\%$ lower cross sections. Self-consistency of the method was checked by resorting to the β group containing contributions from the unresolved $L\beta_1$, $L\beta_3$, $L\beta_4$, and $L\beta_6$ lines arising from filling up vacancies in all three subshells. The production cross sections of the $L\beta$ complex were calculated using the σ_i values derived from the linear system (3) and compared with those directly obtained from the $L\beta$ yield. They were found to be in good agreement with each other. The intensity ratios of the $L\alpha$ and $L\beta_{2,15}$ lines were also tested. Since both transitions arise from vacancies in the L_3 subshell ($2p_{3/2}$), the ratio must be insensitive to the impact energy and must depend exclusively on their radiative widths. The measured values were in good agreement with the theoretical estimates[61] and with the other existing measurements[62] and compilations.[58]

III. RESULTS AND DISCUSSION

The experimental results are displayed in Figs. 2—5 for Ag, In, Sn, and I, respectively. As outlined above, the typical precision is $\sim 5\%$, whereas the absolute magnitude of the experimental data is not estimated to be as accurate due to possible systematic deviations in the efficiency evaluation, the fluorescence yields, and the CK transition rates. In fact, these atomic parameters, calculated for single-vacancy states, implicitly assumed a very low probability for multiple ionization processes. This condition seems to be sufficiently fulfilled in the present case.[63] Furthermore, at low proton velocities the L_1-subshell ionization cross section is comparable with σ_2 and σ_3. As a consequence, the absolute accuracy decreases since the vacancy production in the L_2 and L_3 subshells by CK transitions from the $2s_{1/2}$ level becomes appreciable in comparison with the primary ionization process. Nevertheless, no contribution from this uncertainty was reported on the final values of the ionization cross sections.

The experimental results were compared with the theoretical predictions of the following models: pure PWBA[9]; BEABC, the BEA formulation of Hansen[12] in-

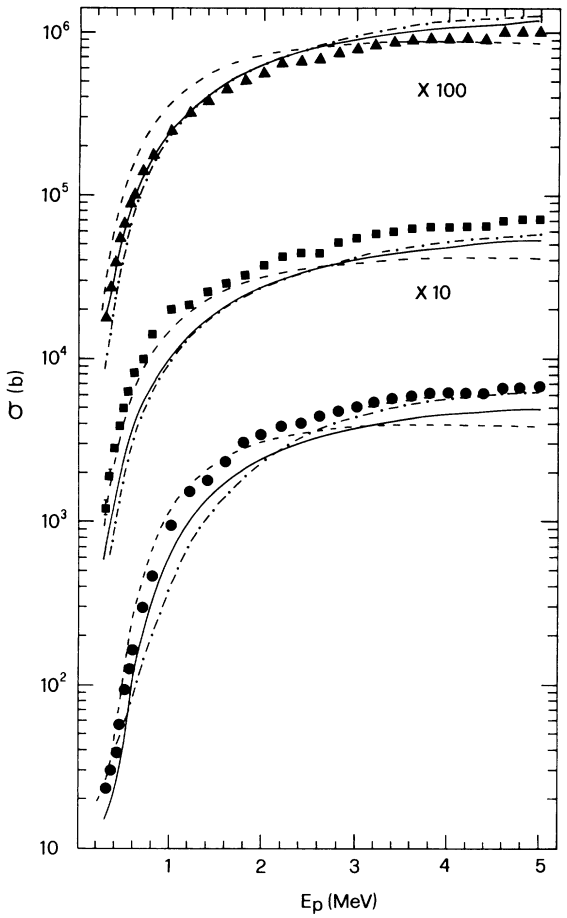

FIG. 2. L-subshell ionization cross sections of Ag compared with theoretical predictions: ●, σ_1; ■, σ_2; ▲, σ_3; ——, ECPSSR; —·—·—·, BEABC; and — — —, SCABR.

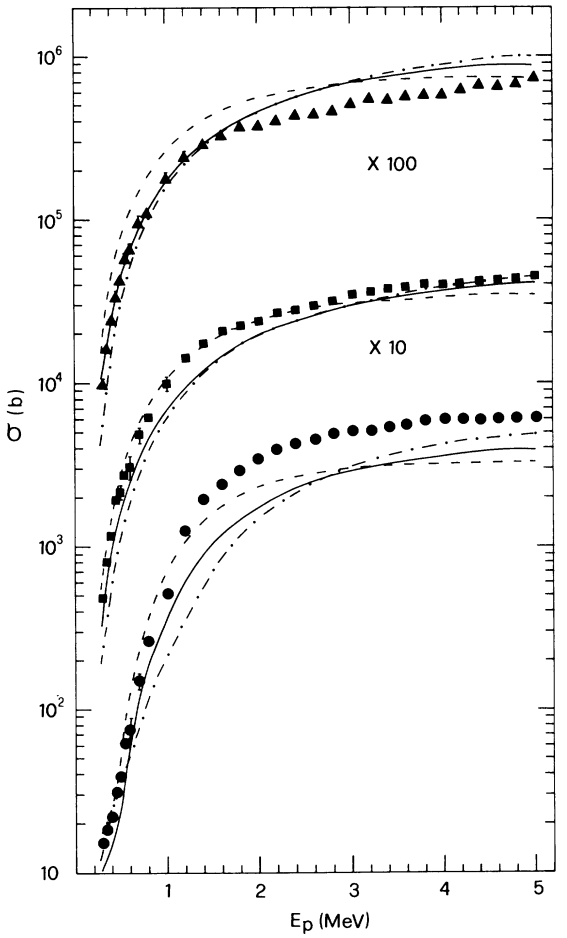

FIG. 3. Same as Fig. 2 but for In.

cluding corrections for the electron binding-energy increase as suggested by Basbas *et al.*,[64] and accounting for the projectile Coulomb retardation by means of the procedure of Ref. 65, since Garcia's proposal[66] turned out to be ineffective; SCABCR, the Aarhus group theory,[13] which takes into account binding and relativistic effects, projectile Coulomb deflection, and energy loss in the ionization process; and ECPSSR,[6] the perturbed—stationary-state theory with energy loss, Coulomb, and relativistic corrections included. Electron capture from the projectile was not included because of the low values of the Z_1/Z_2 charge ratios. The SCABCR predictions were extracted from the tables of Ref. 67. The theoretical calculations relative to PWBA and ECPSSR were performed by using the tabulation of Benka and Kropf[68]; similar results were obtained with the tables of Ref. 69 except for ~15% overestimation at low-velocity regime.

The PWBA overestimates the experimental results typically by ~50% and, therefore, has been discarded. The other models reproduce rather well the magnitude and the overall trend of the data; their predictions are also shown in Figs. 2—5. Focusing upon the experimental results, the following remarks can be made.

(a) Sn and I. The SCABR values are higher than the experimental cross sections up to $E_p \simeq 3.0$ MeV and then become lower. A completely opposite behavior is shown by the BEABC. Instead, the ECPSSR reproduces the magnitude and the energy dependence of the experimental points quite well. As is seen from Fig. 5, the iodine cross sections, particularly σ_1 and σ_2, show some fluctuating behavior. This is most likely due to a not completely correct evaluation of the various line intensities needed for determinating the cross sections. From Fig. 1 it appears that properly extracting the individual line intensities is a rather difficult task. Actually, the complexity of the experimental $AgIO_3$ spectra makes it hard to obtain truly reliable information from the nonlinear least-square-fitting techniques because of the number of peaks which have to be analyzed and the background subtraction. Nevertheless, the experimental results exhibit an overall trend in very good agreement with the theoretical predictions.

(b) Ag; the same remarks are valid for the L_3-subshell ionization cross section of silver, while σ_1 and σ_2 show a large disagreement (~50% in the worst case) with the corresponding theoretical predictions, which are always lower than the experimental results. Two reasons can be invoked to explain this discrepancy. First, these cross sec-

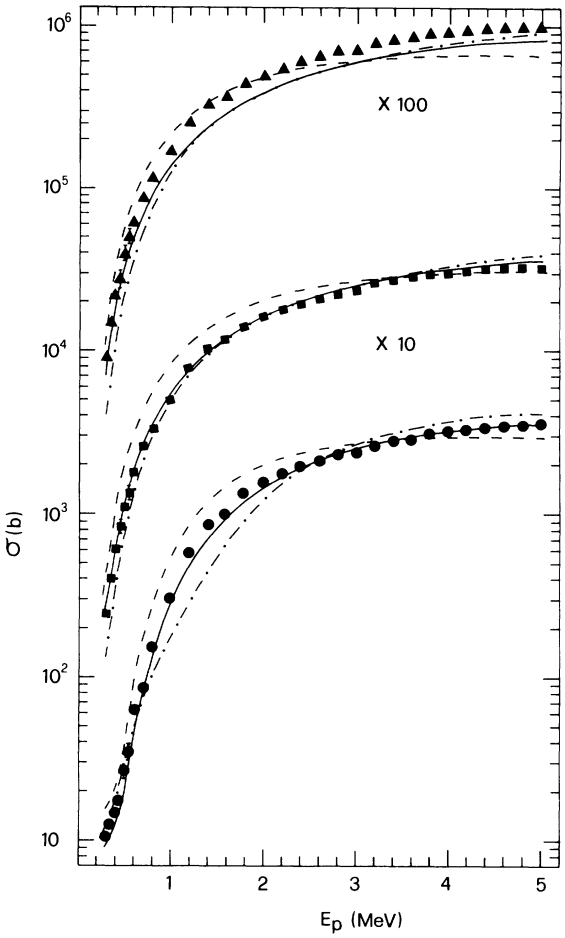

FIG. 4. Same as Fig. 2 but for Sn.

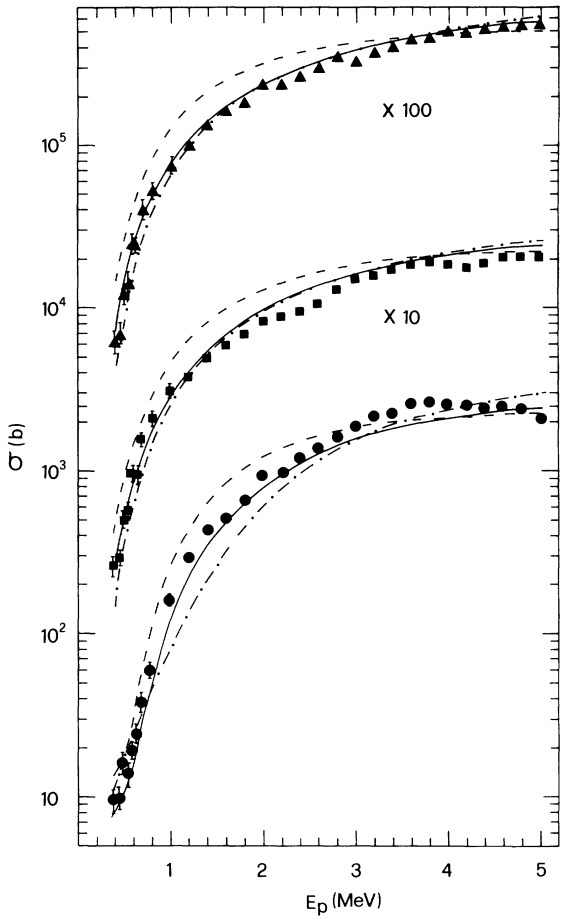

FIG. 5. Same as Fig. 2 but for I.

tions derive from the low-intensity $L\gamma_{1,5}$ and $L\gamma_{2,3}$ lines rising from a large background produced by the $L\alpha$ and $L\beta$ groups in a very compressed spectrum. Second, in this region the slope of the efficiency curve is so steep and critical that little changes can also give rise to big differences. However, the best approximation to the general data behavior is also achieved by the ECPSSR theory in this case.

(c) In; the situation for σ_2 and σ_3 is similar to the one encountered for Sn and I cross sections, whereas σ_1 shows a large discrepancy which cannot be ascribed to some experimental inadequacy. It could most probably be due to some inaccuracy in the adopted atomic parameters. In fact, the L_1-subshell parameters show several discontinuities in accordance with onsets and cutoffs of CK transitions, which represent the dominant component of the L_1 decay rate. The most relevant discontinuities of f_{12}, f_{13}, and ω_1 have been placed just at $Z=49$ owing to the cutoff and the onset of the L_1-$L_3M_{4,5}$ and L_1-$L_2M_{3,4}$ CK transitions, respectively. High-resolution measurements[70] have shown that the experimental Z dependence is somewhat smoother than that predicted by the theory. Actually the experimental results do not show sharp discontinuities, but strongly support the conclusion that the L_1-$L_3M_{4,5}$ CK transition is inoperative for $Z \geq 50$ and 51. Therefore, a correction can be suggested for the observed discrepancy by assuming for the ω_1 fluorescence yield of indium an intermediate value between those relative to cadmium and tin. A phenomenological estimate was obtained, i.e., $\omega_1 \simeq 0.03$, by the least-square method. In this way the experimental points are brought to superimpose to the ECPSSR predictions. Owing to the sum rule of the different deexcitations yields of the $2s_{1/2}$ vacancy, the assumed ω_1 value lowers the f_{12} and f_{13} CK rates and improves the agreement for the σ_1 and σ_2 cross sections, too.

A more stringent test of the different models comes from inspection of the σ_1/σ_2, σ_1/σ_3, and σ_2/σ_3 ratios for $E_p \leq 2.0$ MeV which are displayed in Figs. 6–9 together with the theoretical predictions. The σ_2/σ_3 ratios are a very smooth function of the incident energy, as the wave functions of the $2p_{1/2}$ and $2p_{3/2}$ electrons are similar. On the contrary, the σ_1/σ_2 and σ_1/σ_3 ratios show a well-pronounced energy dependence. The nodal structure of the $2s_{1/2}$ wave function is clearly visible. At low bombarding energies the σ_1/σ_2 and σ_1/σ_3 ratios rise steeply indicating that σ_2 and σ_3 drop more rapidly than σ_1. This can be explained by bearing in mind that the ionization probability becomes more sensitive to the high-momentum

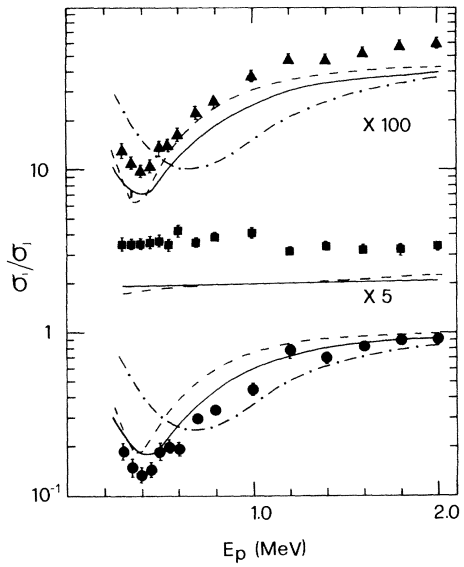

FIG. 6. Experimental and theoretical ratios of Ag L-subshell ionization cross sections: ●, σ_1/σ_2; ■, σ_2/σ_3; ▲, σ_1/σ_3; ——, ECPSSR; —·—·—·, BEABC; and — — —, SCABR.

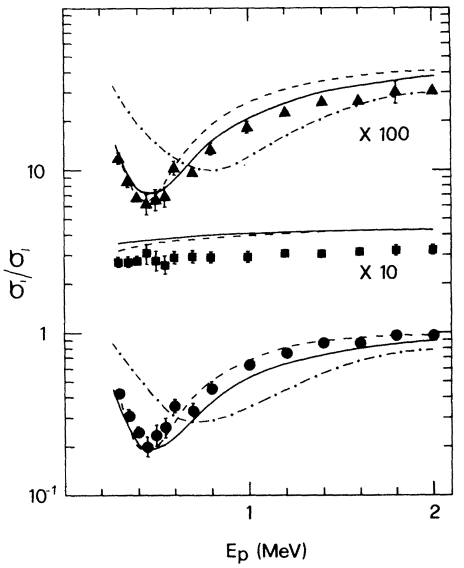

FIG. 8. Same as Fig. 6 but for Sn.

tail of the wave function.

The experimental minima can be located at $E_p \simeq 380$, 430, 460, and 625 keV for Ag, In, Sn, and I, respectively. All these energies lead to the same value of the ratio between the scaled velocity $\eta_L = (v/v_L)^2$ and the scaled binding energy $\theta_{L_i} = 4I_{L_i}/Z^2$ Ry. Here v_L and v are the velocities of the L-shell electrons and projectile, respectively, the I_{L_i} is the ionization energy of the L_i-subshell electrons, the $Z_L = Z_2 - 4.15$ is the effective nuclear charge seen by electron in the L shell, and Ry is the K-shell ionization energy of hydrogen.

The present result $\eta_L/\theta_{L_i} \simeq 0.022$ agrees very well with similar values previously obtained for higher-Z elements[71] and with theoretical estimates. No previous results have been reported on the elements concerned in this work except for the relative measurements on silver of Ref. 62, which are in good agreement with the present data.

With regard to the comparison with the different theories, the following conclusions can be drawn.

(a) σ_2/σ_3 ratios. All the models substantially produce identical estimates of these ratios (the BEABC curves have not been reported as they overlap those relative to the other theories). The theoretical predictions underestimate the experimental results for silver, the tin values are slightly overestimated, while the indium ones show opposite behavior. On the contrary, an excellent agreement is

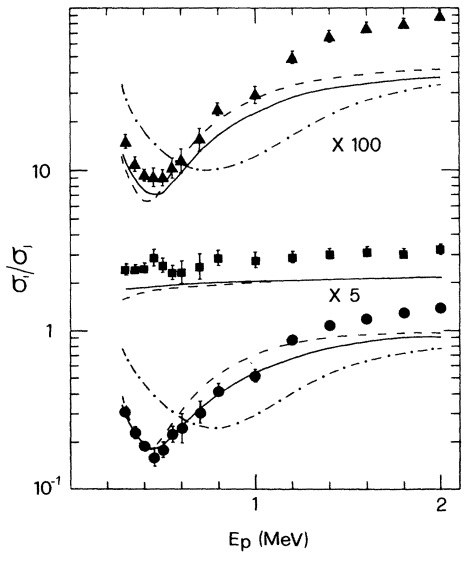

FIG. 7. Same as Fig. 6 but for In.

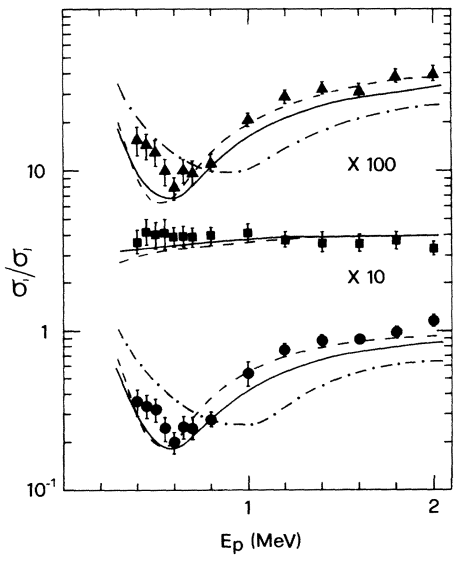

FIG. 9. Same as Fig. 6 but for I.

found for iodine.

(b) The energy minima predicted by BEABC are almost twice as high as the experimental results obtained from σ_1/σ_2 and σ_1/σ_3 ratios. Furthermore, the widths of the BEABC curves are too large. Finally, the agreement between BEABC estimates and measured data is very poor in the region of the kink produced by the node of the $2s$ wave function.

(c) The SCABR predictions are quite accurate and well reproduce the main features of the experimental data. However, the SCA curves, relative to σ_1/σ_2 and σ_2/σ_3 ratios, display minima ~ 25 keV shifted toward lower energy with respect to the experimental values, whereas the widths become narrower than the measured ones.

(d) The ECPSSR predicts very well both the energy position of the minima and their width.

From the above remarks and from the discussion about the individual cross sections it is evident that the best estimates are generally achieved by the ECPSSR, which reproduces quite well all the physical features of the experimental results.

IV. CONCLUSIONS

The measured L-subshell ionization cross sections of Ag, In, Sn, and I in the energy range $0.300 \leq E_p \leq 5.000$ MeV are in good agreement with previous results whenever available. The magnitude and the overall trend are well reproduced by the current theories provided that adequate corrections for binding effect, polarization, relativistic motion of inner-shell electrons, energy loss, and Coulomb deflection of projectile are introduced. Generally the ECPSSR theory provides the best estimates.

These conclusions are confirmed by a more stringent test on the ratios of the subshell ionization cross sections around the critical region of the inflection due to the node of the $2s$ wave function. The energy minima of the σ_1/σ_2 and σ_1/σ_3 ratios are found to be in good agreement with theoretical predictions and with known results for higher-Z elements. Concerning the discontinuity in the atomic parameters of the L_1 subshell, the present results on indium support a Z dependence of the ω_1 fluorescence yield less sharp than that tabulated and suggest an empirical estimate of $\simeq 0.03$.

ACKNOWLEDGMENTS

I wish to thank Dr. R. Palombari and Mrs. A. Cascini for their help in target preparation. The continuous and valuable assistance of Mr. M. Cipriano in running the accelerator is gratefully acknowledged.

[1] *Atomic Inner-Shell Processes,* edited by B. Crasemann (Academic, New York, 1975), Vols. I and II.

[2] *Theories of Inner Shell Ionization by Heavy Particles,* edited by H. Paul (North-Holland, Amsterdam, 1980).

[3] *Methods of Experimental Physics,* edited by P. Richard (Academic, New York, 1980), Vol. 17.

[4] *Inner Shell Ionization by Light Ions,* edited by H. Paul (North-Holland, Amsterdam, 1982).

[5] *1982 IEEE Conference on the Application of Accelerators in Research and Industry,* edited by J. L. Duggan and I. L. Morgan (IEEE, New York, 1983).

[6] W. Brandt and G. Lapicki, Phys. Rev. A 23, 1717 (1981).

[7] H. Paul, Nucl. Instrum. Methods 192, 11 (1982).

[8] H. Paul (private communication).

[9] E. Merzbacher and H. W. Lewis in *Handbuch der Physik,* edited by S. Flügge (Springer, Berlin, 1958), Vol. 34, p. 166.

[10] G. Basbas, W. Brandt, and R. H. Ritchie, Phys. Rev. A 7, 1971 (1973).

[11] A. Kumar and B. N. Roy, J. Phys. B 11, 1435 (1978) and references quoted therein.

[12] J. S. Hansen, Phys. Rev. A 8, 822 (1973) and references quoted therein.

[13] J. U. Andersen, E. Laegsgaard, and M. Lund, Nucl. Instrum. Methods 192, 79 (1982) and references quoted therein.

[14] M. O. Krause, J. Phys. Chem. Ref. Data 8, 307 (1979).

[15] M. H. Chen, B. Crasemann, K. N. Huang, M. Aoyagi, and H. Mark, At. Data Nucl. Data Tables 19, 97 (1977).

[16] M. H. Chen, B. Crasemann, and H. Mark, Phys. Rev. A 24, 177 (1981).

[17] D. H. Madison and E. Merzbacher, in *Atomic Inner-Shell Processes,* edited by B. Crasemann (Academic, New York, 1975), Vol. 1, p. 1.

[18] J. S. Hansen, J. C. McGeorge, D. Nix, W. D. Schmidt-Ott, I. Unus, and R. W. Fink, Nucl. Instrum. Methods 16, 365 (1973).

[19] J. L. Campbell and L. A. McNelles, Nucl. Instrum. Methods 125, 205 (1975).

[20] H. E. Lewis, B. E. Simmons, and E. Merzbacher, Phys. Rev. 91, 943 (1953).

[21] S. Messelt, Nucl. Phys. 5, 435 (1958).

[22] R. C. Jopson, H. Mark, and C. D. Swift, Phys. Rev. 127, 1612 (1962).

[23] W. T. Ogier, G. J. Lucas, J. S. Murray, and T. E. Holzer, Phys. Rev. 134A, 1070 (1964).

[24] K. Shima, J. Makino, and J. Sakisaka, J. Phys. Soc. Jpn. 30, 611 (1971).

[25] D. V. Ferree, Ph.D. thesis, University of Tennessee, 1975 (unpublished).

[26] G. A. Bissinger, S. M. Shafroth, and A. W. Waltner, Phys. Rev. A 5, 2046 (1972).

[27] J. Lin, J. L. Duggan, and R. F. Carlton, in *Proceedings of the International Conference on Inner-Shell Ionization Phenomena and Future Applications,* edited by R. W. Fink, S. T. Manson, M. Palms, and P. V. Rao (U.S. AEC, Oak Ridge, Tennessee, 1972), p. 988.

[28] R. C. Bearse, D. A. Close, J. J. Malanify, and C. J. Umbarger, Phys. Rev. A 7, 1269 (1973).

[29] R. B. Liebert, T. Zabel, D. Milianič, H. Larson, V. Valkovič, and G. C. Phillips, Phys. Rev. A 8, 2336 (1973).

[30] R. Akselsson and T. B. Johansson, Z. Phys. 266, 245 (1974).

[31] F. Folkmann, J. Borggreen, and A. Kjeldgaard, Nucl. Instrum. Methods 119, 117 (1974).

[32] J. L. Duggan, R. P. Chaturvedi, C. C. Sachtleben, and J. Lin (unpublished).

[33]K. Ishii, S. Morita, H. Tawara, H. Haji, and T. Shiokawa, Phys. Rev. A 10, 774 (1974).
[34]N. A. Khelil and T. J. Gray, Phys. Rev. A 11, 893 (1975).
[35]F. Hopkins, R. Brenn, A. R. Whittemore, J. Karp, and S. K. Battacherijee, Phys. Rev. A 11, 916 (1975).
[36]R. P. Chaturvedi, R. M. Wheeler, R. B. Liebert, D. J. Milianič, T. Zabel, and G. C. Phillips, Phys. Rev. A 12, 52 (1975).
[37]Md. Rashiduzzaman Khan, D. Crumpton, and P. E. Francois, J. Phys. B 9, 455 (1976).
[38]E. Koltay, D. Berény, I. Kiss, S. Ricsz, G. Hock, and J. Bacso, Z. Phys. A 278, 299 (1976).
[39]S. R. Wilson, F. D. McDaniel, G. R. Rowe, and J. L. Duggan, Phys. Rev. A 16, 903 (1977).
[40]Md. Rashiduzzaman Khan, A. G. Hopkins, D. Crumpton, and P. E. Francois, X-Ray Spectrum. 6, 140 (1977).
[41]O. Benka and M. Geretschläger, Z. Phys. A 284, 29 (1978).
[42]C. Bauer, R. Mann, and W. Rudolph, Z. Phys. A 287, 27 (1978).
[43]R. Anholt, Phys. Rev. A 17, 983 (1978).
[44]G. von Bonani, C. Stoller, M. Stöckli, M. Surter, and W. Wölfli, Helv. Phys. Acta 51, 272 (1978).
[45]A. Berinde, C. Deberth, I. Neamu, C. Protop, N. Scintei, V. Zoran, M. Dost, and S. Röhl, J. Phys. B 11, 2875 (1978).
[46]C. Magno, M. Milazzo, C. Pizzi, F. Porro, A. Rota, and G. Riccobono, Nuovo Cimento A 54, 277 (1979).
[47]E. Laegsgaard, J. U. Andersen, and F. Høgedal, Nucl. Instrum. Methods 169, 293 (1980).
[48]G. Lapicki, R. Laubert, and W. Brandt, Phys. Rev. A 22, 1889 (1980).
[49]K. Sera, K. Ishii, A. Yamadera, A. Kuwako, M. Kamiya, M. Sebata, S. Morita, and T. C. Chu, Phys. Rev. A 22, 2536 (1980).
[50]P. Cuzzocrea, E. Perillo, E. Rosato, G. Spadaccini, N. De Cesare, and M. Vigilante, Lett. Nuovo Cimento 32, 33 (1981).
[51]M. Dost, S. Hoppenau, J. Kising, S. Röh, and P. Schorn, Phys. Rev. A 24, 693 (1981).
[52]R. K. Rice, F. D. McDaniel, G. Basbas, and J. L. Duggan, Phys. Rev. A 24, 758 (1981).
[53]W. Sarter, H. Mommsen, M. Sarker, P. Schürkers, and A. Weller, J. Phys. B 14, 2843 (1981).
[54]C. Bauer, H. Richter, P. Gippner, R. Mann, W. Rudolph, B. Eckhardt, and K. O. Groeneveld, Z. Phys. A 303, 13 (1981).
[55]A. P. Jesus and J. S. Lopes, Nucl. Instrum. Methods 192, 25 (1982).
[56]E. Rosato, M. Vigilante, N. DeCesare, E. Perillo, and G. Spadaccini, Comput. Phys. Commun. 22, 311 (1981).
[57]S. Aïvazian, *Étude Statistique des Dépendences* (MIR, Moscou, 1970), p. 101.
[58]S. I. Salem, S. L. Panossian, and R. A. Krause, At. Data Nucl. Data Tables 14, 91 (1974).
[59]E. Perillo, E. Rosato, P. Cuzzocrea, N. DeCesare, and G. Spadaccini (unpublished).
[60]M. Sandoli, G. Inglima, E. Perillo, E. Rosato, and G. Spadaccini, Report No. INFN/BE-75/3 (unpublished).
[61]J. H. Scofield, At. Data Nucl. Data Tables 14, 121 (1974).
[62]O. Benka, M. Geretschläger, A. Kropf, H. Paul, and D. Semrad, J. Phys. B 9, 779 (1976).
[63]F. Hopkins, in *Methods of Experimental Physics,* edited by P. Richard (Academic, New York, 1980), Vol. 17, p. 335.
[64]G. Basbas, W. Brandt, and R. Laubert, Phys. Rev. A 17, 983 (1978).
[65]G. Lapicki and W. Losonsky, Phys. Rev. A 20, 481 (1979).
[66]J. D. Garcia, Phys. Rev. A 1, 280 (1971).
[67]J. M. Hansteen, O. M. Johnsen, and L. Kocbach, At. Data Nucl. Data Tables 15, 305 (1975).
[68]O. Benka and A. Kropf, At. Data Nucl. Data Tables 27, 219 (1978).
[69]B. H. Choi, E. Merzbacher, and G. S. Khandelwal, At. Data 5, 291 (1973).
[70]B. L. Doyle and S. M. Shafroth, Phys. Rev. A 19, 1433 (1979).
[71]E. L. B. Justiniano, A. A. G. Nader, N. V. deCastro Faria, G. V. Barros Leite, and A. G. dePinho, Phys. Rev. A 21, 73 (1980).